

# Optical gain characteristics of GaAs based type-II AlAsSb/InGaAs/GaAsSb nanoscale heterostructure for near infrared applications

JAYPRAKASH VIJAY<sup>a, b</sup>, A. K. SINGH<sup>a</sup>, P. K. JAIN<sup>b</sup>, P. A. ALVI<sup>c</sup>, KULWANT SINGH<sup>a</sup>, AMIT RATHI<sup>a,\*</sup>

<sup>a</sup>Department of Electronics and Communication Engineering, Manipal University Jaipur, 303007, Rajasthan, India

<sup>b</sup>Department of Electronics and Communication Engineering, Swami Keshvanand Institute of Technology, Management & Gramothan, Jaipur, Rajasthan, India

<sup>c</sup>Department of Physics, Banasthali Vidyapith, Vanasthali, 304022, Rajasthan, India

In this work, a nanoscale-heterostructure with composition layers AlAsSb/InGaAs/GaAsSb is designed on a GaAs substrate. The associated wavefunctions, dispersion profile, behavior of dipole transition matrix elements and optical gain have been evaluated. The heterostructure is modeled using 6 band  $k \cdot p$  method by solving the  $6 \times 6$  Luttinger-Kohn Hamiltonian. At room temperature, the optical gain of around  $6500 \text{ cm}^{-1}$  is obtained at the 1460 nm wavelength for injected carrier concentration of  $5 \times 10^{12}/\text{cm}^2$ . The effects of the externally applied strain and temperature are also investigated for the possible tuning of optical gain and wavelength in the NIR range.

(Received September 9, 2020; accepted April 7, 2021)

**Keywords:** Optical gain, Heterostructure, Quantum well, Near-infrared,  $k \cdot p$  method

## 1. Introduction

In today's technological landscape, optoelectronic devices such as LASERs, LEDs, optical waveguides and directional couplers are playing a major role in the field of optical communication [1, 2]. Semiconductor lasers are based on semiconductor gain media, where stimulated emission is used to achieve optical gain under the effect of large carrier density. In semiconductor lasers, the foremost concern is a very large effective mass of valence band due to the high asymmetry between the lower and upper conduction band mass of III-V semiconductors which essentially must be as small as possible [3]. Semiconductor lasers can be designed by using heterostructures which involve quantum confinement, varying alloy compositions and mismatching of strain so that one can achieve diverse optical and electronic properties. The laser using the heterojunction i.e. junction of two different materials was first suggested by a German-born physicist Herbert Kroemer [4]. He suggested that using heterostructure the population inversion can be enhanced for stimulated emission. In semiconductor physics, the effective mass approximation is widely used for parameterization of bulk crystals using well known time-independent Schrodinger's equation. Band structure calculations can be done on alloy compositions and strained layers to improve the performance of the device for their application in optical communication. So far, theoretically and experimentally numerous research works have been done in order to develop highly efficient lasing heterostructures based on the type-I (straddling gap) and type-II (staggered gap) energy band alignments. The

energy efficiency of heterostructure lasers can be optimized under the effect of external electric field, temperature and pressure [5-11]. The band alignment and the optical gain calculation for nanoscale  $\text{In}_{0.3}\text{Ga}_{0.7}\text{As}/\text{GaAs}_{0.4}\text{Sb}_{0.6}$  heterostructure has been examined and it has been shown that the optical characteristics of the heterostructure can be altered under the effect of external uniaxial strain due to changes in the effective mass of the valance band [12]. H.K. Nirmal et al. [13] also reported the tunability of the optical gain and emission wavelength with the uniaxial pressure of 2, 5 and 8 GPa respectively. The emitted light polarization TE/TM modes are also sensitive to the external tensile strain due to change in the symmetry of wavefunctions and the possible photonic momentums in the quantum wells [14]. Baile Chen et al. [15] reported that at room temperature addition of Bi composition into InGaAs/GaAsSbBi can extend the lasing wavelength without affecting the peak gain value. Consequently, different approaches for the extension of detection wavelength have been presented which includes strain or pressure effect, by changing the compositions of quantum well layers and by changing the quantum well thickness for MWIR (3–8  $\mu\text{m}$ ), SWIR (1.5–3  $\mu\text{m}$ ), and NIR (0.75–1.5  $\mu\text{m}$ ) applications. A quantum well structure operating in the NIR region finds application in the field of optical fiber communication [16], spectroscopy [17], routine analysis of agricultural and food products for quality control [18], medical science for diagnosing diseases [19] etc.

In this paper, a novel type-II nanoscale heterostructure of AlAsSb/ $\text{In}_{0.59}\text{Ga}_{0.41}\text{As}/\text{GaAs}_{0.53}\text{Sb}_{0.47}$  composition is proposed on GaAs substrate for near-infrared emission.

The optical gain spectrum is calculated using the 6 band  $k \cdot p$  method. In the next section, design parameters and the computational details of the work have been presented.

## 2. Heterostructure design specifications

The proposed AlAsSb/In<sub>0.59</sub>Ga<sub>0.41</sub>As/GaAs<sub>0.53</sub>Sb<sub>0.47</sub> nanoscale heterostructure consists of two quantum wells of p-type In<sub>0.59</sub>Ga<sub>0.41</sub>As material with a barrier of n-type GaAs<sub>0.53</sub>Sb<sub>0.47</sub> followed by the claddings of AlAsSb materials on both side. The whole structure is modeled on the GaAs substrate at room temperature. The materials are chosen owing to their suitability for light generation in NIR wavelength as a requirement. Due to the use of cladding layer, electrons are more confined in the quantum well region. The width of quantum well layer is 2 nm, the width of barrier layer is 4 nm and the cladding width is 10 nm in the designed heterostructure. The width of the layers are selected after several calculations in order to optimize the carrier confinement and effective recombination of charge carriers, which contributes to the improvement in optical gain at the desired NIR wavelengths. The material selections and width of the layers are the critical parameters that affect the design of the heterostructure. The GaAs substrate is chosen as its cost is lower and it has higher thermal strength as compared to InP substrates as used in several recent works. The energy band diagram of the AlAsSb/In<sub>0.59</sub>Ga<sub>0.41</sub>As/GaAs<sub>0.53</sub>Sb<sub>0.47</sub> nanoscale heterostructure with conduction band, valance band and the band offsets is shown in the Fig. 1.

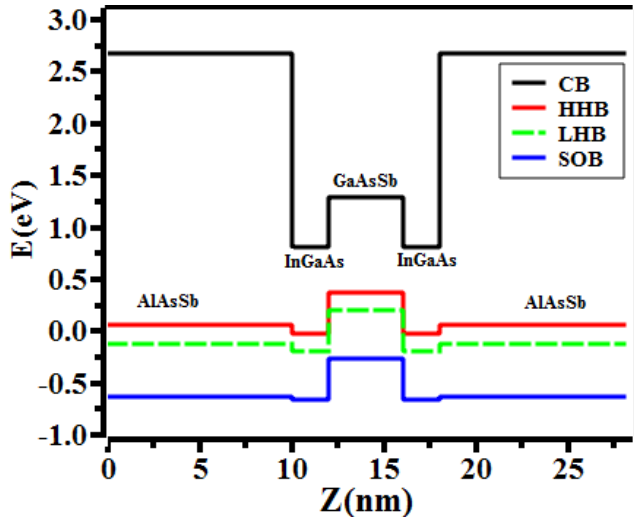


Fig. 1. Energy band diagram of AlAsSb/In<sub>0.59</sub>Ga<sub>0.41</sub>As/GaAs<sub>0.53</sub>Sb<sub>0.47</sub> nanoscale Heterostructure (color online)

The designed heterostructure has the type-II energy band alignment, for the reason that conduction band and valance band of In<sub>0.59</sub>Ga<sub>0.41</sub>As quantum well material is below the conduction band and valance band of GaAs<sub>0.53</sub>Sb<sub>0.47</sub> barrier material respectively. In type-I quantum well structure the conduction band of quantum

well material is below conduction band of the barrier material but the valance band of quantum well material is above valance band of the barrier material. In a semiconductors, effective electronic transition always takes place from the lower part of the conduction band to upper part of valance band. In the designed type-II heterostructure, the transitions will be from the conduction band of In<sub>0.59</sub>Ga<sub>0.41</sub>As material to the valance band of GaAs<sub>0.53</sub>Sb<sub>0.47</sub> material. Due to this reason, type-II heterostructures have smaller bandgap energy and longer emission wavelength. So, the type-II heterostructures are mostly used in design and fabrication of the optoelectronic devices like Lasers, LEDs, couplers and the detectors working at the longer wavelengths. In Fig. 1, the spin orbit split off-band is also shown, but it is far away from the top of the valance band, so it essentially does not participate in effective photonic transitions between conduction and valance bands. The motivation of several recent researchers has been to design heterostructures for obtaining high optical gain at room temperature. Recently, Khan AM et al. [20] have designed a novel type InAlAs/InGaAs/GaAsSb quantum well structure that emits at 1550 nm in the NIR range with the optical gain of 6000/cm. A comparative study with the other heterostructures is also reported in his work, which states that the heterostructure designed in ref. 20 is more favorable to be used for high gain. Optical gain in InGaAsP/GaAsSb QW heterostructure under variable 2D carrier density injection and temperature with a significant improvement in interband optical gain under the effect of external uniaxial strain along [110] has been reported [21].

In order to find the charge carrier confinement in the barrier and well regions,  $6 \times 6$  Luttinger-Kohn Hamiltonian model with the effective-mass approximation has been considered as given in equation (1).

$$H_{6 \times 6}^{LKM}(k) = \begin{pmatrix} H_{3 \times 3}^{LKU} & 0 \\ 0 & H_{3 \times 3}^{LKD} \end{pmatrix} \quad (1)$$

where,  $H_{3 \times 3}^{LKU}$  and  $H_{3 \times 3}^{LKD}$  can be extended as (2) with  $M = U$  or  $D$  signifying upper and lower blocks [22].

$$H_{3 \times 3}^{LKV} = - \begin{pmatrix} P + Q - V_h(z) & \Re(k) \pm iS(k) & \sqrt{2}\Re(k) \pm \frac{i}{\sqrt{2}}S(k) \\ \Re(k) \pm iS(k) & P - Q - V_h(z) & \sqrt{2}Q \pm i\sqrt{\frac{3}{2}}S(k) \\ \sqrt{2}\Re(k) \pm \frac{i}{\sqrt{2}}S(k) & \sqrt{2}Q \mp i\sqrt{\frac{3}{2}}S(k) & P + \Delta_{so} - V_h(z) \end{pmatrix} \quad (2)$$

$$P(k) = \left(\frac{\hbar^2}{2m}\right) \gamma_1(k_t^2 + k_z^2), \quad P(\epsilon) = -a_v(\epsilon_{xx} + \epsilon_{yy} + \epsilon_{zz}) \quad (3a)$$

$$Q(k) = \left(\frac{\hbar^2}{2m}\right) \gamma_2(k_t^2 - 2k_z^2), \quad Q(\epsilon) = -\frac{b}{2}(\epsilon_{xx} + \epsilon_{yy} - 2\epsilon_{zz}) \quad (3b)$$

$$S(k) = \left(\frac{\hbar^2}{2m}\right) \sqrt{3} \left(\frac{\gamma_2 + \gamma_3}{2}\right) k_t^2, \quad \Re(k) = \left(\frac{\hbar^2}{2m}\right) 2\sqrt{3}\gamma_3 k_t k_z \quad (3c)$$

In the Luttinger-Kohn Hamiltonian, equation (2)  $k_t^2 = k_x^2 + k_y^2$   $\gamma_1, \gamma_2$  and  $\gamma_3$  are Luttinger

parameters,  $\epsilon_{xx}$ ,  $\epsilon_{yy}$ ,  $\epsilon_{zz}$  represent strain,  $a_v$  and  $b$  being the Pikus-Bir deformation potentials [23].

Band gap energy, effective mass, valence band and conduction band offsets, elastic stiffness constants, Luttinger parameters and other physical parameters for computation are available [24, 25]. Table 1 shows some of the key parameters of compound semiconductors used in the present study.

Table 1. Compound semiconductor key material parameters

Material	Lattice Constant (Å)	Band Gap (eV)	Effect. mass	$\gamma_1$	$\gamma_2$	$\gamma_3$
GaAs	5.653	1.51	0.067	6.98	2.06	2.93
InAs	6.058	0.41	0.026	20	8.5	9.2
AlAs	5.661	3.09	0.15	3.76	0.82	1.42
AlSb	6.135	2.38	0.14	5.18	1.19	1.97
GaSb	6.095	0.81	0.039	13.4	4.7	6

All the computations in this work have been performed using the Heterostructure Design Studio-v4.0. From the knowledge of the carrier confinement and their positions, the dipole momentum, the optical gain has been determined using the Fermi's golden rule. The six band Hamiltonian for semiconductor includes the spin up and down energy levels of split-off, light and heavy hole bands.

### 3. Results and discussion

In this work, the foremost objective is to study the optical gain characteristics of type-II AlAsSb/In<sub>0.59</sub>Ga<sub>0.41</sub>As/GaAs<sub>0.53</sub>Sb<sub>0.47</sub> nanoscale heterostructure on GaAs substrate at room temperature (300 K). Subsequently, the designed heterostructures have been analyzed to study the dependence of emission wavelength and optical gain on externally applied strain and temperature.

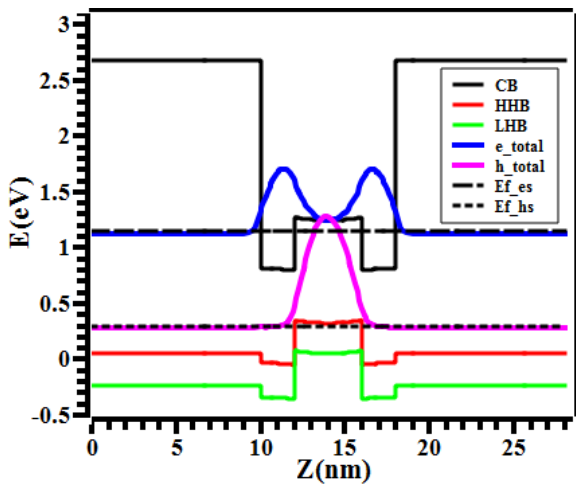


Fig. 2. Net wavefunctions in AlAsSb/In<sub>0.59</sub>Ga<sub>0.41</sub>As/GaAs<sub>0.53</sub>Sb<sub>0.47</sub> nanoscale heterostructure (color online)

To investigate optical characteristics of the heterostructure, primary requirement is to find the energy wavefunctions related with the electrons and holes for which Fermi golden rule is applied [26, 27]. The energy levels related with the holes of valence band and electrons of conduction band can be determined with the help of wavefunctions. The electron and holes wavefunctions for type-II AlAsSb/ In<sub>0.59</sub>Ga<sub>0.41</sub>As/ GaAs<sub>0.53</sub>Sb<sub>0.47</sub> nanoscale heterostructure are shown in Fig. 2 and Fig. 3.

From Fig. 2, it is observed that electrons are highly confined in the quantum well of In<sub>0.59</sub>Ga<sub>0.41</sub>As material while the holes are highly confined in the barrier material GaAs<sub>0.53</sub>Sb<sub>0.47</sub>. So, the total electron density and total hole density are high in the quantum well regions and the barrier region respectively.

Since in the designed type-II heterostructure optical transition will take place from the electrons of the well regions and holes of the barrier region. So, due to large charge carrier density, high optical gain is observed in the heterostructure.

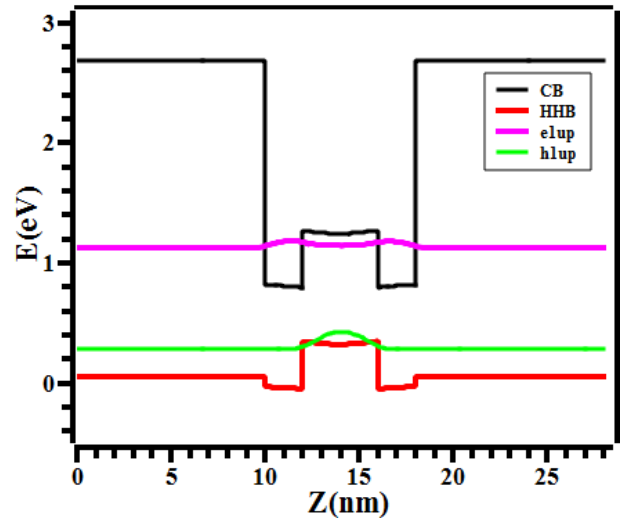


Fig. 3. e1 (up) and h1 (up) wavefunctions in AlAsSb/In<sub>0.59</sub>Ga<sub>0.41</sub>As/GaAs<sub>0.53</sub>Sb<sub>0.47</sub> nanoscale heterostructure (color online)

After the calculation of carrier density in AlAsSb/In<sub>0.59</sub>Ga<sub>0.41</sub>As/GaAs<sub>0.53</sub>Sb<sub>0.47</sub> nanoscale heterostructure, the dispersion curve is plotted for the carriers in both conduction and valence bands. In Fig. 4, the dispersion profile of In<sub>0.59</sub>Ga<sub>0.41</sub>As quantum well with the two energy levels of conduction band electrons (e1 and e2) and three energy levels of the valence band holes (hh1, hh2 and hh3) of GaAs<sub>0.53</sub>Sb<sub>0.47</sub> barrier region are shown.

From the dispersion curve it is observed that conduction band has nearly parabolic profile and has many allowed energy states. It is also observed that the valence band is not parabolic and the heavy holes will have major contribution in the electronic transitions.

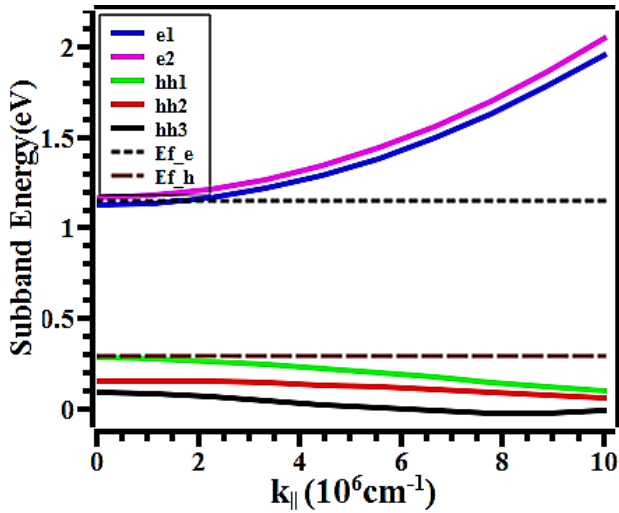


Fig. 4. Dispersion of carrier's energies of AlAsSb/In<sub>0.59</sub>Ga<sub>0.41</sub>As/GaAs<sub>0.53</sub>Sb<sub>0.47</sub> nanoscale heterostructure (color online)

After the calculation of the dispersion profile, the dipole transition elements are computed. In Fig. 5, the behavior of dipole transition elements for AlAsSb/In<sub>0.59</sub>Ga<sub>0.41</sub>As/GaAs<sub>0.53</sub>Sb<sub>0.47</sub> nanoscale heterostructure is shown.

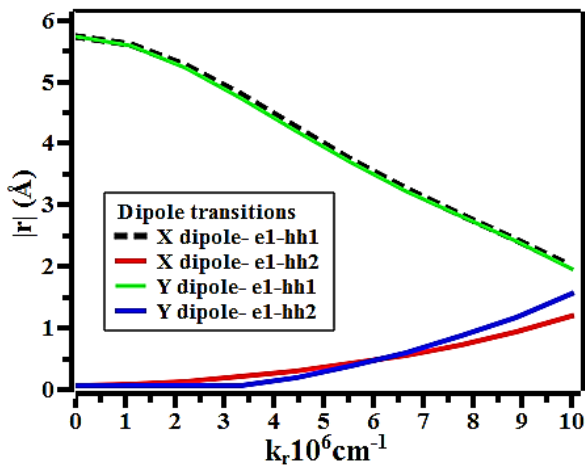


Fig. 5. Dipole transition elements in AlAsSb/In<sub>0.59</sub>Ga<sub>0.41</sub>As/GaAs<sub>0.53</sub>Sb<sub>0.47</sub> nanoscale heterostructure transitions (e1-hh1/e1-hh2) (color online)

The behavior of dipole elements and also the optical gain depends on the polarization mode. In this calculation, the transverse electric (TE) polarization mode is used for the transitions. In TE mode, the optical electric vectors are in the plane of the quantum well layer and the light travels perpendicular to the quantum well. The knowledge of transition dipole elements is required to indicate the transition strength of electrons and holes. It determines the phase vectors related with the electrons and holes for which transitions can occur. The transition strength of carriers does not depend on the direction of interband

transitions, so the strength is identical for the absorption as well emission process. The transition strength depends on the angle between the optical field wave vector and electron wave vector.

In Fig. 5, it is found that for the X-dipole and Y-dipole the strength of the transition e1-hh1 is higher than the transition of e1-hh2. Also, for the greater values of the wave vector, e1-hh1 transition value decreases for both X-dipole and Y-dipole transitions. The higher value of dipole transition of e1-hh1 justifies that most of the optical transitions are for e1-hh1. The knowledge of transition elements is required to calculate the optical gain.

In Fig. 6, a plot between the computed optical gain (/cm) and photonic energy (eV) is shown for AlAsSb/In<sub>0.59</sub>Ga<sub>0.41</sub>As/GaAs<sub>0.53</sub>Sb<sub>0.47</sub> nanoscale heterostructure at room temperature. The maximum optical gain is found of the order of 6500/cm at the photonic energy of 0.85 eV approximately. The relative plot of optical gain and the lasing or emission wavelength for the designed heterostructure is also shown in Fig. 6, which provides the lasing wavelength of 1460 nm of the NIR region. Therefore, the designed novel heterostructure can be used for NIR applications.

A comparative study with the other recently designed heterostructures has been mentioned in table 2, which shows that the designed type-II AlAsSb/In<sub>0.59</sub>Ga<sub>0.41</sub>As/GaAs<sub>0.53</sub>Sb<sub>0.47</sub> nanoscale heterostructure has a higher optical gain and it may act as an alternate choice to be used for NIR applications.

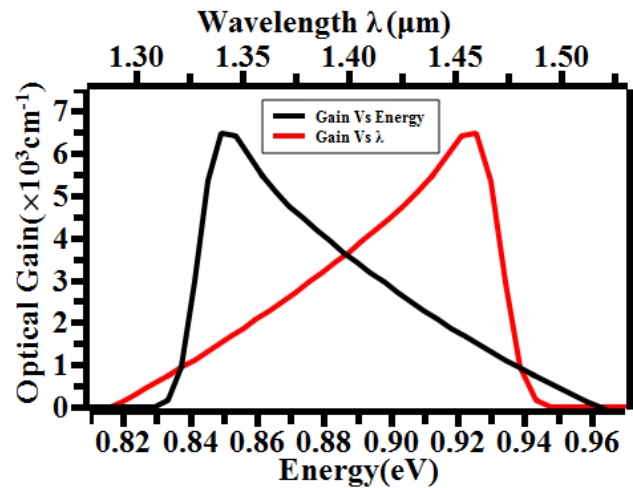


Fig. 6. Optical gain characteristics of AlAsSb/In<sub>0.59</sub>Ga<sub>0.41</sub>As/GaAs<sub>0.53</sub>Sb<sub>0.47</sub> nanoscale heterostructure with radiation wavelength and energy (color online)

To study the tunable optical properties, the designed heterostructure is also modeled under the effect of external strain and temperature. In the last decade, the heterostructure based on strained layers have been studied experimentally and theoretically for optimization of the optical property with renewed interest [34-36]. Further, the research is also on going to achieve the gain and wavelength tunability under the effect of the electric field and temperature [37].

Table 2. Comparison of designed AlAsSb/In<sub>0.59</sub>Ga<sub>0.41</sub>As/GaAs<sub>0.53</sub>Sb<sub>0.47</sub> nanoscale heterostructure with recently designed other nanoscale heterostructures

S. No.	Nanoscale heterostructure	$\lambda$ (nm)	Optical gain (/cm)
1	InAlAs/InGaAs/GaAsSb [20]	1550	6000
2	AlGaAs/GaAsP/AlGaAs [10]	1330	650
3	InAlAs/InGaAs/GaAsSb [28]	1980	1600
4	InGaAsN/GaAs [29]	1300	2100
5	InAs(N)/GaSb [30]	2550	1400
6	InAsN/GaSb [31]	3300	1000
7	InGaAs/GaAsSbBi/GaAs [32]	1610	~2100
8	GaSbBi/GaSb [33]	2700	~3000
9	AlAsSb/InGaAs/GaAsSb [Current work]	1460	6500

It is found that material properties like the lattice constant and bandgap can be altered through the distortion of material electronic structure by providing external pressure, temperature and electric field. To study the tunability of the optical gain for the designed heterostructure the effect of external strain and temperature are investigated. In Fig. 7, a plot between the optical gain and the photonic energy is shown for the designed heterostructure with the strain of 1 GPa, 3 GPa and 5 GPa. On increasing the value of strain, a slight increase in the optical gain due to effective mass mechanism of valance subband (heavy hole) is observed. Also, the lasing wavelength shifts towards the higher values due to a decrease in the effective bandgap of the structure.

Fig. 7 shows the possible tuning range in lasing wavelengths (NIR) and optical gain on applying the external strain (1 GPa, 3 GPa, and 5 GPa) at the room temperature (300 K).

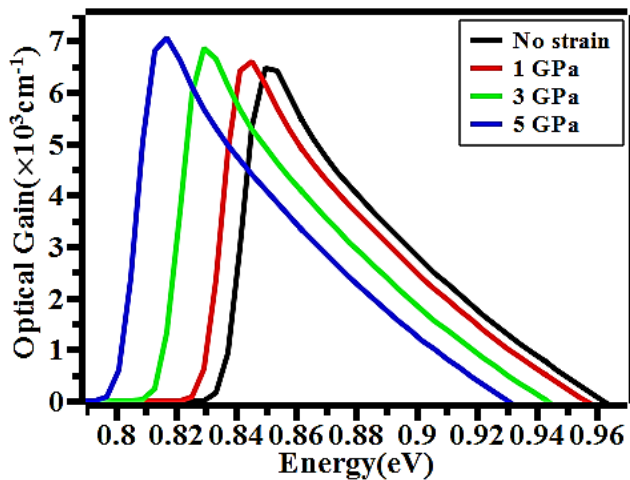


Fig. 7. Optical gain characteristics of AlAsSb/In<sub>0.59</sub>Ga<sub>0.41</sub>As/GaAs<sub>0.53</sub>Sb<sub>0.47</sub> nanoscale heterostructure with different values of external strain (color online)

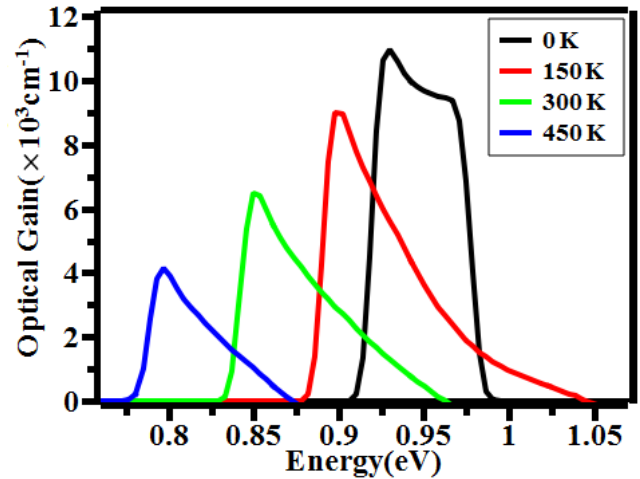


Fig. 8. Optical gain characteristics of AlAsSb/In<sub>0.59</sub>Ga<sub>0.41</sub>As/GaAs<sub>0.53</sub>Sb<sub>0.47</sub> nanoscale heterostructure at different temperature values (color online)

In Fig. 8, a plot between the optical gain and the photonic energy is shown for the designed heterostructure computed at the different temperatures (0 K, 150 K, 300 K and 450 K). It is observed that due to a decrease in temperature optical gain increases and lasing wavelength shifts toward the lower values of the NIR range. So the designed novel type-II AlAsSb/In<sub>0.59</sub>Ga<sub>0.41</sub>As/GaAs<sub>0.53</sub>Sb<sub>0.47</sub> nanoscale hetero-structure shows wideband optical gain and wavelength tunability by changing the external strain and temperature. Hence, due to its tunability and high optical gain, the designed heterostructure is suitable to be used for different NIR applications without changing the material itself.

#### 4. Conclusion

In this paper, GaAs based novel type II-AlAsSb/In<sub>0.59</sub>Ga<sub>0.41</sub>As/GaAs<sub>0.53</sub>Sb<sub>0.47</sub> quantum well structure is theoretically investigated for the calculation of carrier wavefunctions, dispersion profile, dipole transition elements and optical gain. The calculations are based on the 6 band  $k \cdot p$  method by solving the  $6 \times 6$  Luttinger-Kohn Hamiltonian. The optical gain of the order 6500 /cm is obtained at lasing wavelength of 1460 nm for the designed heterostructure at the room temperature. In this work, the tunability of optical gain is also reported in the NIR wavelength range under the effect of external strain and temperature. Consequently, the same quantum well structure can be used for different NIR applications without changing the material itself.

## Acknowledgement

Authors are obliged to Dr. Konstantin I. Kolokolov (F/o Physics, M. V. Lomonosov Moscow State University, Moscow, Russia) for his technical help with the Heterostructure design studio software.

## References

- [1] S. L. Chuang, "Physics of Optoelectronic Devices", Wiley, New York, 1995.
- [2] C. L. Chen, "Elements of Optoelectronics and Fiber Optics" McGraw-Hill Education, Boston, 1996.
- [3] E. Yablonovitch, E. O. Kane, *J. Light. Technol.* **6**(8), 1292 (1988).
- [4] H. Kroemer, *Surf. Sci.* **132**(1-3), 543 (1983).
- [5] E. V. Bogdanov, N. Ya Minina, J. W. Tomm, H. Kissel, *J. Appl. Phys.* **112**(9), 093113 (2012).
- [6] W. W. Bewley, C. L. Felix, E. H. Aifer, I. Vurgaftman, L. J. Olafsen, J. R. Meyer, H. Lee, R. U. Martinelli, J. C. Connolly, A. R. Sugg, G. H. Olsen, M. J. Yang, B. R. Bennett, B. V. Shanabrook, *Appl. Phys. Lett.* **73**, 3833 (1998).
- [7] H. K. Nirmal, N. Yadav, F. Rahman, P. A. Alvi, *Superlattices Microstruct.* **88**, 154 (2015).
- [8] H. Zhu, N. Song, T. Lian, *J. Am. Chem. Soc.* **133**, 8762 (2011).
- [9] P. A. Alvi, *Mater. Sci. Semicond. Process* **31**(1), 106 (2015).
- [10] M. Riyaj, A. K. Singh, A. Rathi, S. Kattayat, S. Kumar, S. Dalela, P. A. Alvi, *Optik* **181**, 389 (2019).
- [11] M. P. Semtsiv, M. Wienold, S. Dressler, W. T. Masselink, G. Fedorov, D. Smirnov, *Appl. Phys. Lett.* **93**, 071109 (2008).
- [12] A. K. Singh, M. Riyaj, S. G. Anjum, N. Yadav, A. Rathi, M. J. Siddique, P. A. Alvi, *Superlattices Microstruct.* **98**, 406 (2016).
- [13] H. K. Nirmal, N. Yadav, S. Dalela, A. Rathi, M. J. Siddiqui, P. A. Alvi, *Physica E Low Dimens. Syst.* **80**, 36 (2016).
- [14] E. V. Bogdanov, H. Kissel, K. Kolokolov, N. Ya. Minina, *Semicond. Sci. Technol.* **31**(3), 035008 (2016).
- [15] B. Chen, *Opt. Express* **25**(21), 25183 (2017).
- [16] S. Addanki, I. S. Amiri, P. Yupapin, *Results Phys.* **10**, 743 (2018).
- [17] C. Pasquini, *Anal. Chim. Acta* **1026**, 8 (2018).
- [18] J. U. Porep, D. R. Kammerer, R. Carle, *Trends Food Sci. Technol.* **46**(2), 211 (2015).
- [19] Y. Li, T. Wang, Y. Liu, Y. Xu, Z. Sun, *J. Drug. Deliv. Sci. Technol.* **53**(1), 101156 (2019).
- [20] A. M. Khan, M. Sharma, M. I. Khan, S. Kattayat, G. Bhardwaj, M. A. Samak, S. H. Saeed, P. A. Alvi, *Optik* **183**, 842 (2019).
- [21] A. K. Singh, A. Rathi, M. Riyaj, G. Bhardwaj, P. A. Alvi, *Superlattices Microstruct.* **111**(1), 591 (2017).
- [22] Chih-Sheng Chang, Shun Lien Chuang, *IEEE J. Sel. Top. Quantum Electron.* **1**(2), 218 (1995).
- [23] G. L. Bir, G. E. Pikus, "Simmetriya i deformatsionnye efekty v poluprovodnikakh (Symmetry and Strain-Induced Effects in Semiconductors)" Wiley, New York, Engl., 1974.
- [24] I. Vurgaftman, J. R. Meyer, L. R. Ram-Mohan, *J. Appl. Phys.* **89**(11), 5815 (2001).
- [25] J. Hu, X. G. Xu, J. A. H. Stotz, S. P. Watkins, A. E. Curzon, M. L. W. Thewalt, N. Matine, C. R. Bolognesi, *Appl. Phys. Lett.* **73**(19), 2799 (1998).
- [26] H. Paul, "Quantum Wells, Wires and Dots: Theoretical and Computational Physics of Semiconductor Nanostructures", John Wiley & Sons, 2005.
- [27] J. Vijay, R. K. Yadav, P. A. Alvi, K. Singh, A. Rathi, *Mater. Today* **30**(1), 128 (2020).
- [28] C. H. Pan, C. P. Lee, *J. Appl. Phys.* **113**, 043112 (2013).
- [29] K. Sandhya, G. Bhardwaj, R. Dolia, P. Lal, S. Kumar, S. Dalela, F. Rahman, P. A. Alvi, *Opto-Electronics Review* **26**, 210 (2018).
- [30] A. B. Ahmed, H. Saidi, S. Ridene, H. Bouchriha, *2015 IEEE J. Quantum Electron.* **51**(5), 1 (2015).
- [31] M. Debbichi, A. Ben Fredj, A. Bhourri, M. Saïd, J-L. Lazzari, Y. Cuminal, A. Joullié, Philippe Christol, *Mater. Sci. Eng. C* **28**(5-6), 751 (2008).
- [32] B. Chen, *Optics Express* **25**(21), 25183 (2017).
- [33] I. Ammar, N. Sfina, M. Fnaiech, *Mater. Sci. Eng. B* **266**, 115056 (2021).
- [34] S. Gupta, F. Rahman, M. J. Siddiqui, P. A. Alvi, *Physica B Condens. Matter.* **411**, 40 (2013).
- [35] J. Vijay, K. Singh, D. Soni, A. Rathi, *IOP Conf Ser: Mater. Sci. Eng.* **594**, 012002 (2019).
- [36] H. K. Nirmal, S. G. Anjum, P. Lal, A. Rathi, S. Dalela, M. J. Siddiqui, P. A. Alvi, *Optik* **127**, 7274 (2016).
- [37] R. Dolia, G. Bhardwaj, A. K. Singh, S. Kumar, P. A. Alvi, *Superlattices Microstruct.* **112**, 507 (2017).

\*Corresponding authors: amitrathi1978@gmail.com